1 **Interaction of zero-valent iron and carbonaceous materials for reduction of**
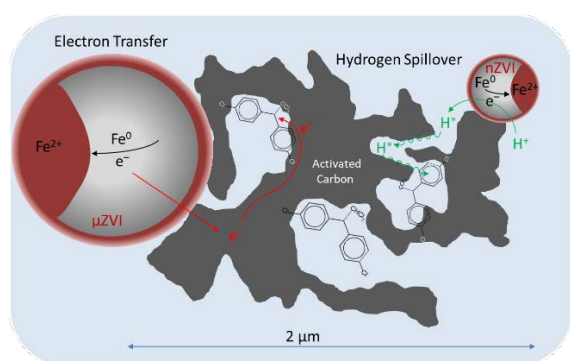
2 **DDT**

3 Frank-Dieter Kopinke*, Sarah Sühnholz, Anett Georgi and Katrin Mackenzie

4 Helmholtz Centre for Environmental Research – UFZ, Department of Environmental

5 Engineering, D-04318 Leipzig, Germany

6 *Corresponding author. Fax: +49 341235451234.

7 *E-mail address:* frank-dieter.kopinke@ufz.de

8 GRAPHICAL ABSTRACT

9

10 **ABSTRACT**

11 Dechlorination of dichlorodiphenyltrichloroethane (DDT) as a model compound was

12 performed with zero-valent iron (micro-ZVI and nano-ZVI) as reductant and

13 carbonaceous adsorbents as sink and catalyst in water. DDT is rapidly converted to

14 dichlorodiphenyldichloroethane (DDD) in direct contact with ZVI. However, up to 90%

15 of the DDD is transformed into non-identified, most likely oligomeric products. There is

16 no indication of dechlorination at the aromatic rings. DDT is still rapidly dechlorinated

17 when it is adsorbed on carbonaceous adsorbents, even though ZVI particles have no

18 direct access to the adsorbed DDT. The carbonaceous materials function as adsorbent

19 and catalyst for the dechlorination reaction at once. From electrochemical experiments,

20   we deduced that direct physical contact between ZVI particles and the adsorbent is

21   essential for enabling a chemical reaction. Electron conduction alone does not effect

22   any dechlorination reaction. We hypothesize hydrogen species (H*) which spill from

23   the ZVI surface to the carbon surface and initiate reductive transformations there. The

24   role of carbonaceous adsorbents is different for different degradation pathways: in

25   contrast to hydrodechlorination (reduction), adsorption protects DDT from

26   dehydrochlorination (hydrolysis).

27

28   *Keywords:* Dechlorination, Zero-valent iron, DDT, Spill over, Hydrolysis

29

30   **1. Introduction**

31   Zero-valent iron (ZVI) is a powerful reductant in remediation technologies (Phenrat

32   et a., 2019; Fu et al., 2014; Raychoudhury and Scheytt, 2013; Miehr et al., 2004). It can

33   chemically reduce a variety of environmental pollutants, such as chlorinated organic

34   compounds, including chlorinated methanes and ethenes (Fennelly and Roberts,

35   1998; Arnold and Roberts, 2000; Wang and Farrell, 2003). The dominant reaction in

36   aqueous media is a hydrodechlorination according to $Fe^0 + R\text{-}Cl + H_2O \rightarrow Fe^{2+} + R\text{-}H$

37    $+ Cl^- + OH^-$. Usually, ZVI is used as micro-ZVI (μZVI, $d_{particle}$ = 1-100 μm) or as nano-

38   ZVI (nZVI, $d_{particle}$ = 20-100 nm). Despite its many environmentally benign properties,

39   ZVI has also some limitations and shortcomings, among them a relatively low sorption

40   affinity for nonpolar organic pollutants (Dries et al., 2004; Burris et al., 1998, 1995;

41   Allen-King et al., 1997). This affects the overall efficiency of chemical reactions on iron

42   surfaces. More importantly, ZVI is not able to degrade a number of chlorinated organics

43   at viable rates, such as dichloromethane, 1,2-dichloroethane, chlorobenzene etc.

44   (Andrieux et al., 1986; Fennelly and Roberts, 1998). The low sorption affinity of iron

45 oxide surfaces for organic pollutants can be compensated for by combination of ZVI

46 with carbon-based adsorbents, such as activated carbon (AC) or graphite, yielding a

47 promising new class of reactive materials (Vogel et al., 2019; Guan et al., 2015;

48 Amezquita-Garcia et al., 2013; Su et al., 2013; Yang et al., 2012, 2010a; Tseng et al.,

49 2011; Chang et al., 2011; Sunkara et al., 2011, 2010; Choi et al., 2009a, 2009b, 2008).

50 Carbo-Iron™ is one representative of this class (Mackenzie et al., 2012, 2008; Bleyl et

51 al., 2012). However, adsorption can affect reaction rates either positively or negatively:

52 (i) enrichment of the target pollutants in close vicinity to the chemical reagent, giving

53 rise to enhanced degradation rates, or (ii) protection of the same pollutants from

54 chemical degradation by entrapment in sorption sinks, where they are not accessible

55 to chemical attack (Dries et al. 2004). When chemical reactions take place on

56 carbonaceous surfaces they may play the role of a catalyst rather than a reagent. This

57 can effect reaction rates and product selectivities.

58   The present study investigates the interplay between adsorption and ZVI driven

59 dechlorination in the presence of various carbon-based adsorbents with DDT (1,1'-

60 (2,2,2-trichloro-1,1-ethanediyl)bis(4-chlorobenzene)) as target compound. DDT has a

61 number of features which make it a suitable target for this study: (i) it is of significant

62 environmental concern (Rani et al., 2017), (ii) DDT has aliphatic and aromatic carbon-

63 chlorine bonds in the same molecule which allow direct comparison of reactivities, (iii)

64 there are several studies on DDT degradation in the literature with widely divergent

65 results which are in need of clarification (Ding et al., 2019; Ortiz and Velasco, 2019;

66 Khunita et al., 2019; Zhu et al., 2016; Han et al., 2016; El-Temsah et al., 2016, 2013a,

67 2013b; Singh and Bose, 2015; Poursaberi et al., 2012; Yang et al., 2010b; Cao et al.,

68 2010; Tian et al., 2009; Pirnie et al., 2006; Satapanajaru et al., 2006a, 2006b; Merica

69 et al., 1999; Sayles et al., 1997), and (iv) DDT is highly hydrophobic (log K_{OW} = 6.36)

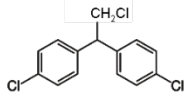70 (Schwarzenbach et al., 2003) and can thus be efficiently removed from aqueous
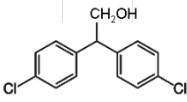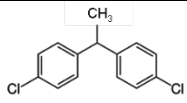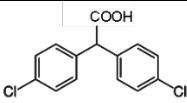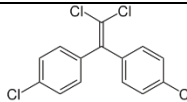
71 matrices by adsorption on carbonaceous materials. This poses the question: can DDT

72 be degraded by chemical reactions in the adsorbed state where it is not in contact with

73 particulate reductants such as ZVI? After answering this question positively, the issues

74 of reaction mechanisms and transferable reactive species – electrons or hydrogen

75 species – are discussed. Finally, the effect of adsorption on AC on the competition

76 between DDT reduction and hydrolysis is considered.

77   From the methodological point of view, DDT's low aqueous solubility (5 µg L^{-1})

78 (Pontolillo and Eganhouse, 2001; Paschke et al., 1998) challenges the experimenter

79 with respect to its speciation and analytics. We are not aware of any previous study in

80 which DDT degradation has been investigated starting below its water solubility

81 concentration. In the present study we did not oversaturate the water phase by DDT,

82 neither did we add co-solvents (Tian et al., 2009; Lowry and Johnson, 2004) nor

83 surfactants (Satapanajaru et al., 2006a, 2006b; Merica et al., 1999; Sayles et al.,

84 1997). We kept the initial DDT concentration strictly below its maximum water solubility.

85   It is useful and common practice in the literature to address the members of the

86 DDT family having the same carbon backbone with their abbreviations. Table 1 gives

87 an overview of chemical structures and frequently used abbreviations for the DDX

88 family.

89 **Table 1.** Chemical structures and common abbreviations for DDT and its metabolites.

Abbreviation	Formula	Abbreviation	Formula
DDT		DDMU	
DDD		DDNU	
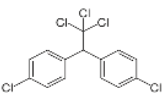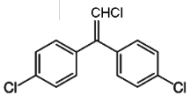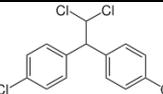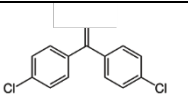
DDMS	CH_2Cl	DDOH	CH_2OH
DDNS or DD0	CH_3	DDA	$COOH$
DDE		DDX	Sum of the DDT-derived metabolites

90

2. A more detailed inspection of literature findings for DDT degradation

92 The reductive degradation of DDT in environmental compartments has generated

93 wide interest in the recent scientific literature (Khunita et al., 2019; Rani et al., 2017;

94 Han et al., 2016; Zhu et al., 2016; and refs. cited there). Nevertheless, a number of

95 significant issues remain open, some of which are briefly reported here on the basis of

96 selected literature studies.

97 Sayles et al. (1997) were the first who investigated the dechlorination of DDT, DDD,

98 and DDE by ZVI in aqueous suspension. The applied initial DDT concentration ($C_{0,DDT}$

99 = 120 µM) was about 4 orders of magnitude above its water solubility (S_{DDT}). This

100 means that all apparent reaction kinetics were affected by the DDT crystal sizes and

101 their dissolution rates. The mass balance of DDX was incomplete (<50 mol-% total

102 recovery). All investigated DDX compounds disappear from aqueous suspensions with

103 similar rates. Such a similarity in rate constants is hardly plausible for chemically

104 controlled rates [6] and is in contrast to the results of the present study (k_{DDT} : k_{DDD} :

105 $k_{DDE} \approx 500 : 1 : \leq 0.2$). DDD, when investigated as a separate feedstock ($C_{0,DDD}$ =

106 12 µM), disappeared from the aqueous ZVI suspension, but no GC-detectable

107 products were found. This is in conformity with our observations.

108   Tian et al. (2009) discussed two DDT reaction pathways with nZVI: (i) electron

109   transfer yielding DDE (dehydrochlorination pathway), and (ii) H transfer yielding DDD

110   as intermediate (hydrodechlorination pathway). If this distinction holds, the H transfer

111   pathway dominates over the electron transfer pathway in all of our ZVI-based reaction

112   systems, including DDT adsorbed on porous adsorbents, because DDD but not DDE

113   is the dominant primary product from DDT. A careful inspection of the experimental

114   data reveals a large gap ($\geq$70%) in the mass balance between disappearing DDT and

115   the sum of detected products (DDD + DDE).

116   Poursaberi et al. (2012) described a complete hydrodechlorination of DDT with nZVI

117   in acidic aqueous suspension ($C_{0,DDT} > S_{DDT}$, $pH_0 = 2$), yielding diphenylethane as the

118   only detectable final reaction product. This is one of the few studies wherein a rapid

119   scission of $C_{aromatic}$-Cl bonds by ZVI has been not only claimed, but also substantiated

120   on the basis of detected reaction products. We attempted to repeat the key

121   experiments according to Poursaberi's protocol, but failed to detect diphenylethane

122   (Kopinke and Balda, 2019). There are strong chemical arguments against a complete

123   dechlorination of benzene rings by undoped ZVI (Martin et al., 2016; Rajeshwar and

124   Ibanez, 1997; Wiley et al., 1991). In contrast, polychlorinated biphenyls may be

125   reactive for partial dechlorination (Ševců et al., 2017; Liu et al., 2016, 2010; Chen et

126   al., 2014; Zhuang et al., 2011; Lowry and Johnson, 2004; Wang and Zhang, 1997).

127   Recently, El-Temsah et al. (2016) investigated the DDT degradation with two types

128   of nZVI at $C_{0,DDT} \gg S_{DDT}$. DDT disappeared rapidly from its aqueous crystal

129   suspension, forming DDD and DDE as intermediates, which disappeared in turn with

130   similar rates. No final reaction products were identified.

131

132   **3. Materials and methods**

133

3.1. Materials

135   Details regarding the materials used including ZVI and carbonaceous adsorbents

136   are provided in the SI part (chapter 1). The sorbents were spiked from an acetone

137   stock solution of DDT (1 g L^{-1}) by shaking them overnight in the minimum amount of

138   solvent. The acetone was then slowly evaporated under nitrogen gas flow, yielding

139   DDT loadings from 0.1 wt-% on graphite up to 0.5 wt-% on AC.

140

3.2.   Experiments with initially dissolved DDT

142   130 mL of aqueous 3 mM bicarbonate solution were spiked with 100 µL stock

143   solution containing DDT and fluoranthene (as an internal standard) in acetone, yielding

144   initial concentrations of 5 µg L^{-1} each. The spiked solution was warmed up to about

145   40°C and shaken for a few minutes in order to ensure complete dissolution of spiked

146   DDT. It was then spiked at ambient temperature with 100 g of µZVI as a pre-activated

147   aqueous suspension (pH = 8.0-8.5, cf. SI part, chapter 2) under argon purging. The

148   250-mL-reaction vessel was filled up to a final water volume of 150 mL. 10 reaction

149   vessels were prepared in the same way. They were shaken end-over-end for defined

150   reaction periods from 5 min to 3 d. All experiments were conducted as duplicates at

151   ambient temperature, i.e. at (22 ± 2)°C.

152   Preliminary experiments were conducted in order to elucidate the speciation of DDT

153   in the reaction bottles. The separation of the reaction mixture after 5 min of contact

154   time (sedimentation of µZVI + decantation of the aqueous phase) revealed that ≥90%

155   of DDT (inclusive rapidly formed DDD) was present on the iron sediment, indicating a

156   fast and almost complete adsorption of dissolved DDT on the ZVI surface. DDT

157   adsorption on glass walls and the PTFE-lined septum was found to be negligible. More

158   details are presented in the SI part (chapter 4).

159

160   *3.3. Experiments with non-agitated reactants: DDT on activated carbon felt (FAC)*

161   *embedded in a fixed bed of µZVI*

162   50 mg of FAC was loaded with 0.5 wt-% of DDT from an acetone stock solution by

163   equilibration for >48 h followed by slow evaporation of the solvent. 10 g of µZVI was

164   pre-activated and dispersed in 40 mL of 3 mM aqueous bicarbonate solution. The 50

165   mg FAC was added as a single slice (1 x 2 cm^2) to the iron suspension, purged for a

166   few minutes with an argon flow and then allowed to precipitate. The FAC was tightly

167   embedded in the µZVI packing (pH of the supernatant 8.5). 5 vials were prepared in

168   this way. After certain periods of contact time without any agitation of the packing (up

169   to 24 h), the FAC was withdrawn, washed with deionized water (to remove adhering

170   iron particles) and extracted for 1 h by 5 mL of a methanol/toluene(1:4)-mixture.

171

172   *3.4. Electrochemical cell experiments*

173   In order to distinguish between different reaction mechanisms, µZVI and FAC were

174   spatially separated but electrically connected (Figure 2). The DDT-impregnated FAC

175   sample (100 mg FAC, 0.5 wt-% DDT) was encapsulated in (i) an open glass tube (d_i =

176   10 mm x length = 50 mm) or (ii) a closed dialysis tubing (Carl Roth, Germany, cut-off

177   150 kDa, d_i = 25 mm x length = 50 mm x wall thickness = 18 µm), and electrically

178   contacted via a steel wire with the µZVI bed. The glass tube was terminated at both

179   ends with loose plugs of glass wool. The steel wire connecting the FAC sample with

180   an ampere-meter was electrically isolated from the ZVI bed by a thin PTFE tubing. The

181   FAC capsules were filled with the same electrolyte as used in the µZVI bed (3 mM

182   NaHCO$_3$). They were permeable for the electrolyte and all kinds of dissolved species

183   but impermeable for µZVI particles. After 24 h of electrical contacting, the FAC

184 capsules were removed, purged with water and extracted with 10 mL of a

185 methanol/toluene(1:4)-mixture.

186

187 *3.5. Experiments with agitated reactants: DDT on suspended adsorbents*

188   100 mg of graphite powder loaded with 0.1 wt-% of DDT were mixed with 40 g of

189 pre-activated µZVI in 20 mL of 3 mM aqueous bicarbonate solution (pH = 8.8). The

190 glass vials were shaken end-over-end for defined reaction periods up to 10 d. The

191 graphite and µZVI particles were then separated using an external magnet. The

192 aqueous graphite suspension was extracted with 5 mL of toluene, containing pyrene

193 as an internal standard. The extract was filtered (PTFE, 0.45 µm), dried over Na_2SO_4

194 and analysed by means of GC-MS. The same procedure was applied to DDT adsorbed

195 on colloidal AC (0.5 wt-% DDT).

196

197 *3.6. Extraction of DDT from aqueous suspensions*

198   Usually, DDT and its organic reaction products were extracted from aqueous

199 suspensions by shaking the entire reaction bottles (250 mL) containing water (150 mL),

200 µZVI (100 g) and sorbents with 10 mL of toluene as extractant on an end-over-end

201 shaker for various time periods. Two internal standards were applied: fluoranthene in

202 the aqueous suspension and pyrene in the extraction solvent. The extraction of DDT

203 raises the question of its chemical stability under multi-phase extraction conditions in

204 the presence of µZVI. Therefore, the extraction procedures were carefully evaluated.

205 Two requirements were found to be essential: (i) we applied a magneto-separation

206 step which separates carbon and iron particles prior to extraction. (ii) ZVI suspensions

207 were acifidified in a second extraction step in order to open oxide/hydroxide surface

208 layers. A detailed description of the optimized extraction procedures is given in the SI

209 part (chapter 3).

210

3.7. Analytical methods

Aliquotes of the organic extracts of aqueous samples were dried over Na_2SO_4, pre-concentrated by solvent evaporation, and analyzed by means of GC-MS (QP 2010 ultra from Shimadzu, HP-5MS capillary column, 30 m x 0.32 mm x 0.25 µm) in SIM and SCAN modes (m/z = 45-400 amu, T_{GC} = 50°C (1 min), 10 K min^{-1} up to 280°C (15 min)). 1 µL of toluene extract was injected in the split mode (1:10, T_{inj} = 230°C). The detection limit of DDT (S/N ≥ 3) from aqueous solution analyzed according to this procedure was about 0.02 µg L^{-1}.

219

4. Results and discussion

Initial experiments were specifically designed to elucidate the speciation of DDT in aqueous solution and recovery by various extraction procedures. Data are presented in the SI part (chapters 3 and 4). We learnt from these data that toluene extraction of the aqueous µZVI suspensions at alkaline conditions (pH = 8.5 to 9) may not always be sufficient for complete recovery of analytes. However, a temporary acidification which dissolves the iron oxide/hydroxide layers around the ZVI core enables their release into the solvent phase.

228

4.1. Experiments with initially dissolved DDT in the absence of carbonaceous adsorbents

Experiments with 'truly dissolved' DDT in aqueous suspensions are difficult to conduct due to its very low aqueous solubility and consequently its high tendency to adsorb rapidly onto surfaces. Thus, we found that even for an initial DDT concentration of 1 µg L^{-1}, the addition of µZVI (667 g L^{-1}) gave rise to fast and almost complete adsorption (> 95% within 5 min) and partial conversion of DDT on the iron surface.

236   We observed that DDT in direct contact with µZVI is rapidly dechlorinated (60 to

237   80% conversion in about 5 min) forming DDD ($\geq$ 90% yield), which is slowly degraded

238   further yielding DDMS (1% after 1 h) and DDNS (0.5% after 1 h). A more detailed DDX

239   product pattern is presented in Table S1. Unsaturated products such as DDE, DDMU

240   and DDNU were not detected. Obviously, hydrodechlorination dominates over

241   dehydrochlorination as reaction pathway (Scheme 1). Diphenylethane was not

242   detected in any experiment, indicating that dechlorination at the benzene ring is

243   beyond the reduction power of ZVI.

244

245   → Please insert Scheme 1 here.

246

247   The observed initial DDT dechlorination rate (with $k_{DDT,\mu ZVI} \approx$ 10-20 h^{-1}) can be

248   converted into apparent second-order rate coefficients $k_{DDT,\mu ZVI,2nd} \approx$ 15-30 L kg^{-1} h^{-1}

249   and normalized to the ZVI surface area (SA) $k_{DDT,\mu ZVI,SA} \approx$ 0.1 L m^{-2} h^{-1}. These values

250   are likely to be lower limits of the true chemical rate coefficients. After 3 d of contact

251   time, about 1% of the initial DDT and only 6% of the initially formed DDD (with $k_{DDD,\mu ZVI}$

252    $\approx$ 0.04 h^{-1}) were still extractable. All other DDX products were only detectable at a

253   trace level. The question of the fate of DDD on the iron surface will be considered later.

254   The concentration of DDE as impurity in DDT ($\leq$1 mol-%) did not change significantly

255   during the first hour of contact with µZVI. After 3 d, about 60% of the DDE was still

256   detectable. This indicates that its reactivity is several orders of magnitude lower than

257   that of DDT, and at least a factor of 5 lower than that of DDD.

258   In a series of experiments, µZVI was replaced by nZVI. These data are presented

259   in the SI part (chapter 5). Surface-normalized rate coefficients for dechlorination of

260   DDT and DDD were found to be similar for nZVI and µZVI. Table S3 gives a summary

261 of rate constants for conversion of DDX compounds in direct or indirect contact with

262 ZVI, determined in the the present study.

263

264 *4.2.   Experiments with non-agitated reactants: DDT adsorbed on activated carbon*

265 *felt in direct contact with a fixed bed of µZVI*

266   In the second part of this study, the reactivity of DDT adsorbed on the inner surface

267 of porous adsorbents such as AC is considered. In this arrangement, no direct contact

268 between adsorbates in the pores and externally attached µZVI particles was possible.

269 If a chemical conversion should take place, chemical reactivity must be transferred

270 from µZVI to adsorbates by means of mobile species. The most probable candidates

271 are electrons or reactive H-species (H*). (Kopinke et al., 2016; Tang et al., 2011; Oh

272 et al., 2002; Li and Farrell, 2001 and references cited there). The nature of H* is not

273 yet fully understood, but H-species able to long-range migration across the surface of

274 metal catalysts and catalyst carriers are well known in the literature (e.g. Prins, 2012).

275 Alternatively, one could hypothesize a certain mobility of adsorbed DDT enabling its

276 diffusion from the inner pores to the external surface of AC. This explanation was

277 carefully checked but disproved (see SI part, chapter 6). Figure 2 shows the setup for

278 the following fixed-bed experiments.

279   The reduction of DDT adsorbed on FAC (0.5 wt-% DDT) which was embedded in a

280 fixed bed of µZVI particles (non-encapsulated FAC slice in Figure 2) follows a first-

281 order kinetics with an apparent rate constant of $k_{DDTonFAC,\mu ZVI} = 0.175$ h^{-1} (inset in Figure

282 1). The first-order kinetics indicates that either (i) all the adsorbed DDT is equally

283 available to the reducing species or (ii) the DDT is sufficiently mobile on the AC surface

284 to reach the preferred reduction sites. Figure 1 shows the FAC extract composition

285 along the reaction time. The overall mass balance is closed with (105 ± 7) mol-%. Note

286   that the fixed bed remains static, meaning that the contact points between FAC fibers

287   and iron particles are not refreshed during the reaction time.

288

289   → Please insert Figure 1 here.

290

291   The data in Figure 1 allow some insights into the reaction pathways (see also SI

292   part, chapter 7). The DDE concentration remains almost constant over the reaction

293   period. Thus it is neither formed nor converted significantly under reaction conditions.

294   This is remarkable with respect to the high chemical reactivity of chlorinated ethenes

295   with ZVI as reductant (Phenrat et al., 2019; Liu et al., 2005; Arnold and Roberts, 2000)

296   as well as with ZVI/carbon composites (Vogel et al., 2019; Kopinke et al., 2016; Su et

297   al., 2013; Tang et al. 2011; Tseng et al. 2011). Chemical reasons for this behavior are

298   discussed in the later paragraph 'Reactivity of DDE'.

299

300   *4.3.   Experiments with non-agitated reactants: DDT adsorbed on activated carbon*

301   *felt in electrical contact with a fixed bed of µZVI*

302   Reducing species transferred from µZVI to the FAC can be electrons or mobile

303   hydrogen species. The following experiment was designed to further elucidate their

304   roles. FAC loaded with DDT (0.5 wt-%) was either in direct contact with µZVI (Figure

305   2, right vial) or connected only electrically with the fixed bed while the DDT-loaded FAC

306   was either placed in the glasswool-plugged tube or in a dialysis tubing (Figure 2, left

307   setup). Actually, the two electrochemical setups shown together in Figure 2 (left part)

308   were carried out in separate vials.

309

310   → Please insert Figure 2 here.

311

312   The electrical resistance between the iron bed and the central point of the FAC

313   was about 100 Ω. When the wire from the FAC was connected to the amperemeter,

314   an electrical current ran between the iron bed (anode) and the embedded FAC

315   (cathode). It decreased steadily from initially 100 µA to about 30 µA after 24 h. We

316   attribute this charge transfer to the polarization of the FAC surface ($Fe^0 \rightarrow Fe^{2+} + 2e^-$

317   and $AC + e^- \rightarrow AC^-$). The transferred charge corresponds to about 50 µmol electrons.

318   This amount is much larger than the amount of adsorbed DDT (1.4 µmol). After 24 h

319   of electrical contacting with the iron bed, the FAC capsules were withdrawn, purged

320   with water and extracted as described above. The GC-MS analyses revealed no

321   significant DDT conversion for DDT on FAC in the dialysis tubing (<0.5 mol-%

322   products) and a very low conversion for DDT on FAC in the glass tube (about 1 mol-%

323   DDD). However, the possibility cannot be completely ruled out that a small amount of

324   µZVI particles may have penetrated the glasswool plugs at the ends of the glass tube,

325   such that they indeed came into direct contact with the FAC. This could possibly

326   explain the low extent of reductive dechlorination. Note that 98.5% of DDT was

327   converted within 24 h when the FAC was in direct contact with the iron bed.

328   We conclude from these electrochemical experiments that the direct physical

329   contact between µZVI particles and the carbonaceous adsorbent is an essential

330   requirement for the reduction of adsorbates such as DDT, and probably other

331   chlorinated compounds. This poses the question: if the transfer of electrons from µZVI

332   to the carbon matrix is not sufficient for reductive dechlorination, which other processes

333   and species are involved? We hypothesize hydrogen species (H*) which spill from the

334   ZVI surface to the carbon surface and initiate reductive transformations there (Tang et

335   al., 2011; Oh et al., 2002). If their spillover is made impossible by breaking the surface

336   contact, the chemical reaction is suspended. Our experimental findings are in

337   conformity with the spillover phenomenon hypothesized in Kopinke et al. (2016) for

338 the dechlorination of TCE adsorbed on AC by nZVI. A similar approach using an

339 electrochemical cell has been applied by Ding and Xu (2016) for the sulfide-driven

340 reduction of DDT, DDD and DDE adsorbed on graphite powder in aqueous

341 suspension. All three DDX compounds were converted when sulfide was in direct

342 contact with the graphite particles, whereas DDT and DDD were not converted when

343 sulphide was electrically connected but spatially separated from the graphite.

344 Obviously, reduction of DDT and DDD needs direct access for sulfur species. Sole

345 delivery of electrons from the graphite matrix is insufficient. This finding is again in

346 conformity with our results on ZVI-driven DDT reduction.

347

348 *4.4.   Experiments with agitated reactants: DDT adsorbed on suspended activated*

349 *carbon particles*

350 In a number of experiments, FAC was replaced by suspended AC particles (d_{50} =

351 1.0 µm) as DDT carriers in order to change the quality of the contact between the

352 reactive particles, from a static to a highly dynamic contacting. Independent of the

353 particle size, DDT adsorbed deeply in AC pores will practically not come into direct

354 contact with µZVI particles. Hence, any chemical reaction between DDT and µZVI has

355 to be mediated by the AC matrix.

356 DDT adsorbed on colloidal AC is converted rapidly in suspension with µZVI ($C_{\mu ZVI}$ =

357 667 g L^{-1}), forming DDD as the main product. 95% DDT conversion within 1 h results

358 in a first-order rate constant of $k_{DDTonAC,\mu ZVI} \approx 3$ h^{-1}. This is an order of magnitude faster

359 than the reduction of DDT on FAC in static contact with µZVI ($k_{DDTonFAC,\mu ZVI}$ = 0.175 h^{-}

360 ^{1}). The higher rate constant is possibly due to the smaller size of the carbon particles

361 (d_{50} = 1.0 µm vs. d_{carbon_fibre} = 12 µm). The DDT conversion kinetics with AC colloids is

362 too fast to be properly resolved in time with the applied batch suspension/extraction

363   technique. The observed conversion rate is comparable to that when DDT is brought

364   into direct contact with suspended µZVI in the absence of AC ($k_{DDT,µZVI} \approx$ 10-20 h^{-1}).

365   In addition to DDD, small fractions of DDMU (0.8% of $C_{0,DDT}$), DDNU (0.4%), DDMS

366   (0.3%) and DDNS (0.5%) were detected. DDD disappears slowly from the reaction

367   mixture with a half-life of about 500 h ($k_{DDDonAC,µZVI} \approx$ 10^{-3} h^{-1}) and without any

368   detectable product pattern.

369   A larger fraction of DDE (about 25%) was already formed by dehydrochlorination of

370   DDT during the loading procedure on AC. Its concentration remained almost constant

371   up to 10 d reaction time in suspension with µZVI, with an uncertainty of ±10%. This

372   results in an upper limit for its reaction rate constant of $k_{DDEonAC,µZVI} \leq 4 \cdot 10^{-4}$ h^{-1}. This is

373   at least 4 orders of magnitude slower than the conversion of DDT.

374

375   *4.5. Dechlorination of DDT adsorbed on suspended graphite particles*

376   DDT (0.1 wt-%) adsorbed on graphite particles ($d_{particle}$ = 1-2 µm) is also rapidly

377   dechlorinated by contact with µZVI in aqueous suspension (Figure 3). The initial rate

378   constant amounts to about $k_{DDTon\_graphite,µZVI} \approx$ 0.1 h^{-1} up to 95% DDT conversion. This

379   value is a factor of 30 smaller than observed for DDT on colloidal AC ($k_{DDTonAC,µZVI} \approx$ 3

380   h^{-1}). Since the electron conductivity of graphite is higher than that of AC, the higher

381   chemical reactivity of DDT adsorbed on AC compared to graphite points to rate-

382   controlling steps other than electron transfer.

383   DDE does not show a significant reactivity even under these favorable reaction

384   conditions ($k_{DDEon\_graphite,µZVI} <$ 10^{-3} h^{-1}). DDD is clearly the main product from DDT,

385   accompanied by minor products of deeper reduction, such as DDMS and DDNS. No

386   significant DDD disappearance was observed within 10 d (<10%). These findings

387   suggest that the adsorbent graphite protects DDD from further reduction. In the

388   absence of graphite, DDD would be converted with a half-life of about 6 h in the

389 presence of 2 kg L^{-1} μZVI. The yield of DDNS is much higher on graphite (8%)

390 compared to AC (0.5%). This comparison shows that the nature of the adsorbent

391 significantly affects the competition between several reduction pathways, in this case

392 partial vs. total hydrodechlorination (i.e. formation of DDD vs. DDNS) in Scheme 1.

393

394 → Please insert Figure 3 here.

395

396 *4.6. Reactivity of DDE*

397 DDE was found to be much less reactive than DDT towards ZVI-driven reduction.

398 This statement holds for pure ZVI as well as for reactions at the surface of

399 carbonaceous adsorbents such as graphite and ACs. This ranking in reactivities is

400 different from that known for aliphatic chlorinated hydrocarbons, where trichloroethene

401 ($k_{TCE,nZVI} = 1.4 \cdot 10^{-2}$ L m^{-2} h^{-1}) (Liu et al., 2005) was found to be much more reactive

402 than chloroform ($k_{CF,nZVI} = 5 \cdot 10^{-4}$ L m^{-2} h^{-1}) (Feng and Lim, 2005).

403 However, this comparison does not take into account two characteristic features of

404 the DDE molecule: (i) the electronic stabilization of the double bond in DDE, whereby

405 its cross-conjunction with two aromatic rings possibly makes it less reactive, and (ii)

406 the DDE molecule has a planar structure due to its conjugated π-electron systems,

407 which determines its mode of adsorption on surfaces and consequently its reactivity in

408 surface reactions. It is not unlikely that the formation of iron-chlorine bonds as a pre-

409 stage of a dechlorination reaction (Wang and Farrell, 2003; Arnold and Roberts, 2000;

410 Andrieiux et al., 1986) is significantly impeded for DDE compared to non-conjugated

411 chloroethenes.

412 It is worth mentioning that DDE was found to be much more reactive than DDT and

413 DDD under conditions where only electrons but no H-species were delivered to a

414 graphite adsorbent (Ding and Xu, 2016). This finding supports our view that H-species

415 play a key role in ZVI/carbon systems, because DDE was found to be less reactive

416 there.

417

418 *4.7. Final reaction products from reductive DDT degradation*

419 The dominant primary product of reductive DDT degradation under all conditions is

420 DDD. However, the DDX mass balance becomes incomplete when DDD is converted

421 further. The expected products of a stepwise hydrodechlorination of DDD, namely

422 DDMS and DDNS, were only detected in low yields or not at all. There was no

423 indication of ring-dechlorinated products, such as diphenylethane. Up to 90 mol-% of

424 the DDD products were missing with µZVI. This poses the question of the fate of the

425 DDT backbone in the presence of ZVI. Obviously, the missing products are not

426 accessible to conventional GC-MS analysis. Therefore, we applied two additional

427 analytical techniques: (i) LC-MS, and (ii) in-source thermodesorption/pyrolysis MS (IS-

428 TD/Py-MS). The latter method is able to detect volatile compounds and decomposition

429 products from non-volatile substrates up to molecular weight (MW) of 1000 g mol^{-1} (cf.

430 SI part, chapter 9). Neither LC-MS nor IS-TD/Py-MS produced indications of additional,

431 potentially higher-MW products from DDT transformation.

432 In conclusion, we are aware of a large mass-balance gap in the reduction pathway

433 of DDT beyond DDD which is also common to most of the literature studies on this

434 topic (Tian et al., 2009; Sayles et al., 1997; Satapanajaru et al., 2006a, 2006b) but

435 mostly not explicitly addressed. In the end, it is hard to evaluate a degradation

436 technique (reduction with ZVI) where the final products are not identified.

437 Considering possible reaction routes, one common feature applies for all saturated

438 members of the DDX group: they have a highly reactive tertiary C-H bond which could

439 be the target of H abstraction. The resulting tertiary benzyl-type radical $Ph_2RC \cdot$ can be

440   assumed to be long-living, i.e. subject of buildup reactions. Higher-MW hydrocarbons,

441   although still chlorinated, may be considered as part of a detoxification approach.

442

443   *4.8. Reduction vs. hydrolysis of DDT*

444   Beside hydrodechlorination, DDT is subject of dehydrochlorination (β-elimination

445   of HCl, cf. Scheme 1) yielding DDE under environmental conditions (Roberts et al.,

446   1993). As we could show, DDE is less reactive towards reduction by ZVI than DDT and

447   DDD. Therefore, 'hydrolysis' of DDT to DDE is counterproductive with respect to its

448   reductive degradation. In the present study, we also investigated the effect of DDT

449   adsorption on AC on its hydrolysis rate (for kinetic data see SI part, chapter 10). Briefly,

450   DDT hydrolysis is inhibited due to adsorption on AC by a factor of 500 compared to the

451   homogeneous reaction ($k_{DDT,hom,OH^-}^{25°C} = 1 \cdot 10^{-2}$ M^{-1} s^{-1} (Roberts et al., 1993) vs.

452   $k_{DDT,het,AC,OH^-}^{23°C} = 2 \cdot 10^{-5}$ M^{-1} s^{-1}, this study). This means, adsorption of DDT shifts the

453   competition between hydrodechlorination and dehydrochlorination in favor of the

454   reduction (Mackenzie et al., 2005a, 2005b). This may be considered as an additional

455   positive effect of carbonaceous adsorbents.

456

457

458   **5. Conclusions**

459   All studies reviewed in section 2 describe high reactivities of DDT with various ZVI-

460   based reductants. However, the findings differ largely with respect to the reactivity of

461   the intermediates. In addition, mass balances are typically not closed. Final products

462   of DDT conversion are uncertain. Moreover, the main portion of converted DDT ends

463   up in non-identified, presumbly chlorinated high-MW products. These will be even less

464   water-soluble than DDT itself. Nevertheless, it is hard to assess the environmental

465   impact of non-identified compounds.

466   The present study overcomes some of the addressed shortcomings. We have to

467   admit - in conformity with the literature findings - that the final sink of DDD remains

468   unresolved. DDD reduction to DDMS and DDNS is a major conversion pathway with

469   nZVI (about 75%, cf. SI part, chapter 5) but accounts for only a minor fraction with μZVI

470   (<10%). The main focus of this study was the reactivity of DDT and its metabolites

471   towards μZVI when adsorbed on carbonaceous adsorbents. The results show clearly

472   that DDT is available for the reducing species from μZVI even when it is not accessible

473   for direct contact with the metal particles. Some findings indicate that active hydrogen

474   species rather than electrons are responsible for DDT reduction in the pore space of

475   carbonaceous adsorbents brought into contact with ZVI. Irrespective of the reaction

476   mechanism, the carbonaceous adsorbents play the role of chemical catalysts in the

477   dechlorination reaction: DDT adsorbed on their surface is reductively converted

478   whereby the reductants are delivered from ZVI. There is no need for direct contact

479   between ZVI particles and the DDT substrate.

480   Recently, Pignatello et al. (2017) have reviewed the present state of knowledge

481   about the impact of carbonaceous adsorbents for reactivity of organic compounds in

482   natural and engineered environments. They conclude that sorption can effect both,

483   shielding of contaminants from reaction and mediation of chemical conversion. The

484   present study understands as a contribution for rounding this interplay on hand of the

485   prominent example of DDT and its metabolites.

486

491

492 **Appendix A. Supplementary data**

493   Supplementary data and methodical comments associated with this article can be

494 found in the online version, at http://dx.doi.org …

495

496 **References**

497 Allen-King, R.M., Halket, R.M., Burris, D.R., 1997. Reductive transformation and

498 sorption of cis-and trans-1, 2-dichloroethene in a metallic iron-water system. Environ.

499 Toxicol. Chem. 16, 424-429.

500 Amezquita-Garcia, H., Razo-Flores, E., Cervantes, F., Rangel-Mendez, J., 2013.

501 Activated carbon fibers as redox mediators for the increased reduction of

502 nitroaromatics. Carbon 55, 276-284.

503 Andrieux, C.P., Saveant, J.M., Su, K.B., 1986. Kinetics of dissociative electron

504 transfer. Direct and mediated electrochemical reductive cleavage of the carbon-

505 halogen bond. J. Phys. Chem. 90, 3815-3823.

506 Arnold, W.A., Roberts, A.L., 2000. Pathways and kinetics of chlorinated ethylene and

507 chlorinated acetylene reaction with Fe(0) particles. Environ. Sci. Technol. 34, 1794-

508 1805.

509 Bleyl, S., Kopinke, F.-D., Mackenzie, K., 2012. Carbo-Iron® - Synthesis and

510 stabilization of Fe(0)-doped colloidal activated carbon for in situ groundwater

511 treatment. Chem. Eng. J. 191, 588-595.

512 Burris, D.R., Allen-King, R.M., Manoranjan, V.S., Campbell, T.J., Loraine, G.A.,

513 Deng, B., 1998. Chlorinated ethene reduction by cast iron: sorption and mass

514 transfer. J. Environ. Engin. 124, 1012-1019.

515 Burris, D.R., Campbell, T.J., Manoranjan, V.S., 1995. Sorption of trichloroethylene

516 and tetrachloroethylene in a batch reactive metallic iron-water system. Environ. Sci.

517 Technol. 29, 2850-2855.

518 Cao, F., Li, F., Liu, T., Huang, D., Wu, C., Feng, C., Li, X., 2010. Effect of Aeromonas

519 hydrophila on reductive dechlorination of DDTs by zero-valent iron. J. Agric. Food.

520 Chem. 58, 12366-12372.

521 Chang, C., Lian, F., Zhu, L., 2011. Simultaneous adsorption and degradation of γ-

522 HCH by nZVI/Cu bimetallic nanoparticles with activated carbon support. Environ.

523 Pollut. 159, 2507-2514.

524 Chen, X., Yao, X., Yu, C., Su, X., Shen, C., Chen, C., Huang, R., Xu, X., 2014.

525 Hydrodechlorination of polychlorinated biphenyls in contaminated soil from an e-

526 waste recycling area, using nanoscale zero-valent iron and Pd/Fe bimetallic

527 nanoparticles. Environ. Sci. Technol. 21, 5201-5210.

528 Choi, H., Agarwal, S., Al-Abed, S.R., 2009a. Adsorption and simultaneous

529 dechlorination of PCBs on GAC/Fe/Pd: mechanistic aspects and reactive capping

530 barrier concept. Environ. Sci. Technol. 43, 488-493.

531 Choi, H., Al-Abed, S.R., Agarwal, S., 2009b. Catalytic role of palladium and relative

532 reactivity of substituted chlorines during adsorption and treatment of PCBs on

533 reactive activated carbon. Environ. Sci. Technol. 43, 7510-7515.

534 Choi, H., Al-Abed, S.R., Agarwal, S., Dionysiou, D.D., 2008. Synthesis of reactive

535 nano-Fe/Pd bimetallic system-impregnated activated carbon for the simultaneous

536 adsorption and dechlorination of PCBs. Chem. Mater. 20, 3649-3655.

537   Ding, K., Duran, M., Xu, W.Q., 2019. The synergistic interaction between sulfate-

538   reducing bacteria and pyrogenic carbonaceous matter in DDT decay. Chemosphere

539   233, 252-260.

540   Ding, K., Xu, W., 2016. Black carbon facilitated dechlorination of DDT and its

541   metabolites by sulfide. Environ. Sci. Technol. 50, 12976-12983.

542   Dries, J., Bastiaens, L., Springael, D., Agathos, S.N., Diels, L., 2004. Competition for

543   sorption and degradation of chlorinated ethenes in batch zero-valent iron systems.

544   Environ. Sci. Technol. 38, 2879-2884.

545   El-Temsah, Y.S., Joner, E.J., 2013. Effects of nano-sized zero-valent iron (nZVI) on

546   DDT degradation in soil and its toxicity to collembola and ostracods. Chemosphere

547   92, 131-137.

548   El-Temsah, Y.S., Oughton, D.H., Joner, E.J., 2013. Effects of nano-sized zero-valent

549   iron on DDT degradation and residual toxicity in soil: a column experiment. Plant Soil

550   368, 189-200.

551   El-Temsah, Y.S., Sevcu, A., Bobcikova, K., Cernik, M., Joner, E.J., 2016. DDT

552   degradation efficiency and ecotoxicological effects of two types of nano-sized zero-

553   valent iron (nZVI) in water and soil. Chemosphere 144, 2221-2228.

554   Feng, J., Lim, T.-T., 2005. Pathways and kinetics of carbon tetrachloride and

555   chloroform reductions by nano-scale Fe and Fe/Ni particles: comparison with

556   commercial micro-scale Fe and Zn. Chemosphere 59, 1267-1277.

557   Fennelly, J.P., Roberts, A.L., 1998. Reaction of 1,1,1-trichloroethane with zero-valent

558   metals and bimetallic reductants. Environ. Sci. Technol. 32, 1980-1988.

559 Fu, F.L., Dionysiou, D.D., Liu, H., 2014. The use of zero-valent iron for groundwater

560 remediation and wastewater treatment: A review. J. Hazard. Mater. 267, 194-205.

561 Guan, X., Sun, Y., Qin, H., Li, J., Lo, I.M., He, D., Dong, H., 2015. The limitations of

562 applying zero-valent iron technology in contaminants sequestration and the

563 corresponding countermeasures: the development in zero-valent iron technology in

564 the last two decades (1994-2014). Water Res. 75, 224-248.

565 Han, Y., Shi, N., Wang, H., Pan, X., Fang, H., Yu, Y., 2016. Nanoscale zero-valent

566 iron-mediated degradation of DDT in soil. Environ. Sci. Technol. 23, 6253-6263.

567 Khunita, B.K., Anwar, M.F., Alam. T., Samim, M., Kumari, M., Arora, I., 2019.

568 Synthesis and characterization of zero-valent iron nanoparticles, and the study of

569 their effect against the degradation of DDT in soil and assessment of their toxicity

570 against collembola and ostracods. ACS Omega 18502-18509.

571 Kopinke, F.-D., Speichert, G., Mackenzie, K., Hey-Hawkins, E., 2016. Reductive

572 dechlorination in water: Interplay of sorption and reactivity. Appl. Catal. B: Environ.

573 181, 747-753.

574 Kopinke, F., Balda, M., 2020. Hydrodechlorination of aromatic chlorocompounds in

575 water with zero-valent iron: the role of nickel traces. Chem. Eng. J. 388, article

576 number 1241852020.

577 Li, T., Farrell, J., 2001. Electrochemical investigation of the rate-limiting mechanisms

578 for trichloroethylene and carbon tetrachloride reduction at iron surfaces. Environ. Sci.

579 Technol. 35, 3560-3565.

580   Liu, Y., Majetich, S.A., Tilton, R.D., Sholl, D.S., Lowry, G.V., 2005. TCE

581   dechlorination rates, pathways, and efficiency of nanoscale iron particles with

582   different properties. Environ. Sci. Technol. 39, 1338-1345.

583   Liu, Z., Zhang, F.-S., 2010. Nano-zero-valent iron contained porous carbons

584   developed from waste biomass for the adsorption and dechlorination of PCBs.

585   Biores. Technol. 101, 2562-2564.

586   Liu, Z., Zhang, F., Hoekman, S.K., Liu, T., Gai, C., Peng, N., 2016. Homogeneously

587   dispersed zero-valent iron nanoparticles supported on hydrochar-derived porous

588   carbon: simple, in situ synthesis and use for dechlorination of PCBs. ACS Sustain.

589   Chem. Eng. 4, 3261-3267.

590   Lowry, G.V., Johnson, K.M., 2004. Congener-specific dechlorination of dissolved

591   PCBs by microscale and nanoscale zero-valent iron in a water/methanol solution.

592   Environ. Sci. Technol. 38, 5208-5216.

593   Mackenzie, K., Battke, J., Koehler, R., Kopinke, F.-D., 2005a. Catalytic effects of

594   activated carbon on hydrolysis reactions of chlorinated organic compounds: Part 2.

595   1,1,2,2-Tetrachloroethane. Appl. Catal. B: Environ. 59, 171-179.

596   Mackenzie, K., Battke, J., Kopinke, F.-D., 2005b. Catalytic effects of activated carbon

597   on hydrolysis reactions of chlorinated organic compounds: Part 1. γ-

598   hexachlorocyclohexane. Cat. Today 102, 148-153.

599   Mackenzie, K., Bleyl, S., Georgi, A., Kopinke, F.-D., 2012. Carbo-Iron - An Fe/AC

600   composite as alternative to nano-iron for groundwater treatment. Water Res. 46,

601   3817-3826.

602 Mackenzie, K., Schierz, A., Georgi, A., Kopinke, F.D., 2008. Colloidal activated

603 carbon and carbo-iron - novel materials for in-situ groundwater treatment. Global

604 NEST J. 10, 54-61.

605 Martin, E.T., McGuire, C.M., Mubarak, M.S., Peters, D.G., 2016. Electroreductive

606 remediation of halogenated environmental pollutants. Chem. Rev. 116, 15198-15234.

607 Merica, S.G., Jedral, W., Lait, S., Keech, P., Bunce, N.J., 1999. Electrochemical

608 reduction and oxidation of DDT. Can. J. Chem. 77, 1281-1287.

609 Miehr, R., Tratnyek, P.G., Bandstra, J.Z., Scherer, M.M., Alowitz, M.J., Bylaska, E.J.,

610 2004. Diversity of contaminant reduction reactions by zero-valent iron: Role of the

611 reductate. Environ. Sci. Technol. 38, 139-147.

612 Oh, S.-Y., Cha, D.K., Chiu, P.C., 2002. Graphite-mediated reduction of 2, 4-

613 dinitrotoluene with elemental iron. Environ. Sci. Technol. 36, 2178-2184.

614 Ortiz, I., Velasco, A., 2019. Degradation of DDT, Endrin, and Endosulfan in polluted

615 soils by zero-valent iron (Fe-0) and zero-valent iron-copper (Fe-0-Cu-0) treatments.

616 Revista Mexicana de Ingeneria Quimica 18, 875-888.

617 Paschke, A., Popp, P., Schüürmann, G., 1998. Water solubility and octanol/water-

618 partitioning of hydrophobic chlorinated organic substances determined by using

619 SPME/GC. Fresenius J. Anal. Chem. 360, 52-57.

620 Phenrat, T., Le, T.S.T., Naknakorn, B., Lowry, G.V., 2019. Chemical reduction and

621 oxidation of organic contaminants by nanoscale zero-valent iron. Nanoscale zero-

622 valent iron particles for environmental restoration. Springer, pp. 97-155.

623 Pignatello, J., Mitch, W.A., Xu, W., 2017. Activity and reactivity of pyrogenic

624 carbonaceous matter toward organic compounds. Environ. Sci. Technol. 51, 8893-

625 8908.

626 Pirnie, E.F., Talley, J.W., Hundal, L.S., 2006. Abiotic transformation of DDT in

627 aqueous solutions. Chemosphere 65, 1576-1582.

628 Pontolillo, J., Eganhouse, R.P., 2001. The search for reliable aqueous solubility (Sw)

629 and octanol-water partition coefficient (Kow) data for hydrophobic organic

630 compounds: DDT and DDE as a case study. Water-Resources Investigations Report

631 1, 4201.

632 Poursaberi, T., Konoz, E., Sarrafi, A.M., Hassanisadi, M., Hajifathli, F., 2012.

633 Application of nanoscale zero-valent iron in the remediation of DDT from

634 contaminated water. Chem. Sci. Trans. 1, 658-668.

635 Prins, R., 2012. Hydrogen spillover. Facts and fiction. Chem. Rev. 112, 2714-2738.

636 Rajeshwar, K., Ibanez, J.G., 1997. Environmental electrochemistry: Fundamentals

637 and applications in pollution sensors and abatement. Elsevier.

638 Rani, M., Shanker, U., Jassal, V., 2017. Recent strategies for removal and

639 degradation of persistent & toxic organochlorine pesticides using nanoparticles: a

640 review. J. Environ. Manag. 190, 208-222.

641 Raychoudhury, T., Scheytt, T., 2013. Potential of zero-valent iron nanoparticles for

642 remediation of environmental organic contaminants in water: a review. Water Sci.

643 Technol. 68, 1425-1439.

644 Roberts, A., Jeffers, P., Wolfe, N., Gschwent, P., 1993. Structure-reactivity

645 relationships in dehydrohalogenation reactions of polychlorinated and

646 polybrominated alkanes. Crit. Rev. Environ. Sci. Technol. 23, 1-39.

647 Satapanajaru, T., Anurakpongsatorn, P., Pengthamkeerati, P., 2006a. Remediation

648 of DDT-contaminated water and soil by using pretreated iron byproducts from the

649 automotive industry. J. Environ. Sci. Health B 41, 1291-1303.

650 Satapanajaru, T., Anurakpongsatorn, P., Songsasen, A., Boparai, H., Park, J.,

651 2006b. Using low-cost iron byproducts from automotive manufacturing to remediate

652 DDT. Water, Air, Soil Pollut. 175, 361-374.

653 Sayles, G.D., You, G., Wang, M., Kupferle, M.J., 1997. DDT, DDD, and DDE

654 dechlorination by zero-valent iron. Environ. Sci. Technol. 31, 3448-3454.

655 Schwarzenbach, R.P., Gschwend, P.M., Imboden, D.M., Environmental Organic

656 Chemistry 2nd, ed. John Wiley & Sons: Hoboken, U.S.A. 2003 , pp. 1202 and 165-

657 172.

658 Ševců, A., El-Temsah, Y.S., Filip, J., Joner, E.J., Bobčíková, K., Černík, M., 2017.

659 Zero-valent iron particles for PCB degradation and an evaluation of their effects on

660 bacteria, plants, and soil organisms. Environ. Sci. Technol. 24, 21191-21202.

661 Singh, S.P., Bose, P., 2015. Degradation of soil-adsorbed DDT and its residues by

662 NZVI addition. RSC Advances 5, 94418-94425.

663 Su, Y.-f., Cheng, Y.-l., Shih, Y.-h., 2013. Removal of trichloroethylene by zero-valent

664 iron/activated carbon derived from agricultural wastes. J. Environ. Manag. 129, 361-

665 366.

666   Sunkara, B., Zhan, J., He, J., McPherson, G.L., Piringer, G., John, V.T., 2010.

667   Nanoscale zero-valent iron supported on uniform carbon microspheres for the in situ

668   remediation of chlorinated hydrocarbons. ACS Appl. Mater. Interf. 2, 2854-2862.

669   Sunkara, B., Zhan, J., Kolesnichenko, I., Wang, Y., He, J., Holland, J.E., McPherson,

670   G.L., John, V.T., 2011. Modifying metal nanoparticle placement on carbon supports

671   using an aerosol-based process, with application to the environmental remediation of

672   chlorinated hydrocarbons. Langmuir 27, 7854-7859.

673   Tang, H., Zhu, D., Li, T., Kong, H., Chen, W., 2011. Reductive dechlorination of

674   activated carbon-adsorbed trichloroethylene by zero-valent iron: carbon as electron

675   shuttle. J. Environ. Qual. 40, 1878-1885.

676   Tian, H., Li, J., Mu, Z., Li, L., Hao, Z., 2009. Effect of pH on DDT degradation in

677   aqueous solution using bimetallic Ni/Fe nanoparticles. Sep. Purific. Technol. 66, 84-

678   89.

679   Tseng, H.-H., Su, J.-G., Liang, C., 2011. Synthesis of granular activated carbon/zero-

680   valent iron composites for simultaneous adsorption/dechlorination of

681   trichloroethylene. J. Hazard. Mater. 192, 500-506.

682   Vogel, M., Kopinke, F.-D., Mackenzie, K., 2019. Acceleration of microiron-based

683   dechlorination in water by contact with fibrous activated carbon. Sci. Total Environ.

684   660, 1274-1282.

685   Wang, C.-B., Zhang, W.-X., 1997. Synthesizing nanoscale iron particles for rapid and

686   complete dechlorination of TCE and PCBs. Environ. Sci. Technol. 31, 2154-2156.

687   Wang, J., Farrell, J., 2003. Investigating the role of atomic hydrogen on chloroethene

688   reactions with iron using Tafel analysis and electrochemical impedance

689   spectroscopy. Environ. Sci. Technol. 37, 3891-3896.

690   Wiley, J.R., Chen, E.C.M., Chen, E.S.D., Richardson, P., Reed, W.R., Wentworth,

691   W.E., 1991. The determination of absolute electron-affinities of chlorobenzenes,

692   chloronaphthalenes and chlorinated biphenyls from reduction potentials, J.

693   Electroanal. Chem. 307 (1-2), 169-182.

694   Yang, J., Guo, Y., Xu, D., Cao, L., Jia, J., 2012. A controllable Fe(0)-C permeable

695   reactive barrier for 1,4-dichlorobenzene dechlorination. Chem. Eng. J. 203, 166-173.

696   Yang, J., Cao, L., Guo, R., Jia, J., 2010a. Permeable reactive barrier of surface

697   hydrophobic granular activated carbon coupled with elemental iron for the removal of

698   2,4-dichlorophenol in water. J. Hazard. Mater. 184, 782-787.

699   Yang, S.-C., Lei, M., Chen, T.-B., Li, X.-Y., Liang, Q., Ma, C., 2010b. Application of

700   zero-valent iron (Fe0) to enhance degradation of HCHs and DDX in soil from a

701   former organochlorine pesticides manufacturing plant. Chemosphere 79, 727-732.

702   Zhu, C., Fang, G., Dionysiou, D.D., Liu, C., Gao, J., Qin, W., Zhou, D., 2016. Efficient

703   transformation of DDTs with persulfate activation by zero-valent iron nanoparticles: a

704   mechanistic study. J. Hazard. Mater. 316, 232-241.

705   Zhuang, Y., Ahn, S., Seyfferth, A.L., Masue-Slowey, Y., Fendorf, S., Luthy, R.G.,

706   2011. Dehalogenation of polybrominated diphenyl ethers and polychlorinated

707   biphenyl by bimetallic, impregnated, and nanoscale zero-valent iron. Environ. Sci.

708   Technol. 45, 4896-4903.

709

710   List of figure captions:

711

712   **Scheme 1.** Reaction pathways of DDT in aqueous suspension with µZVI.
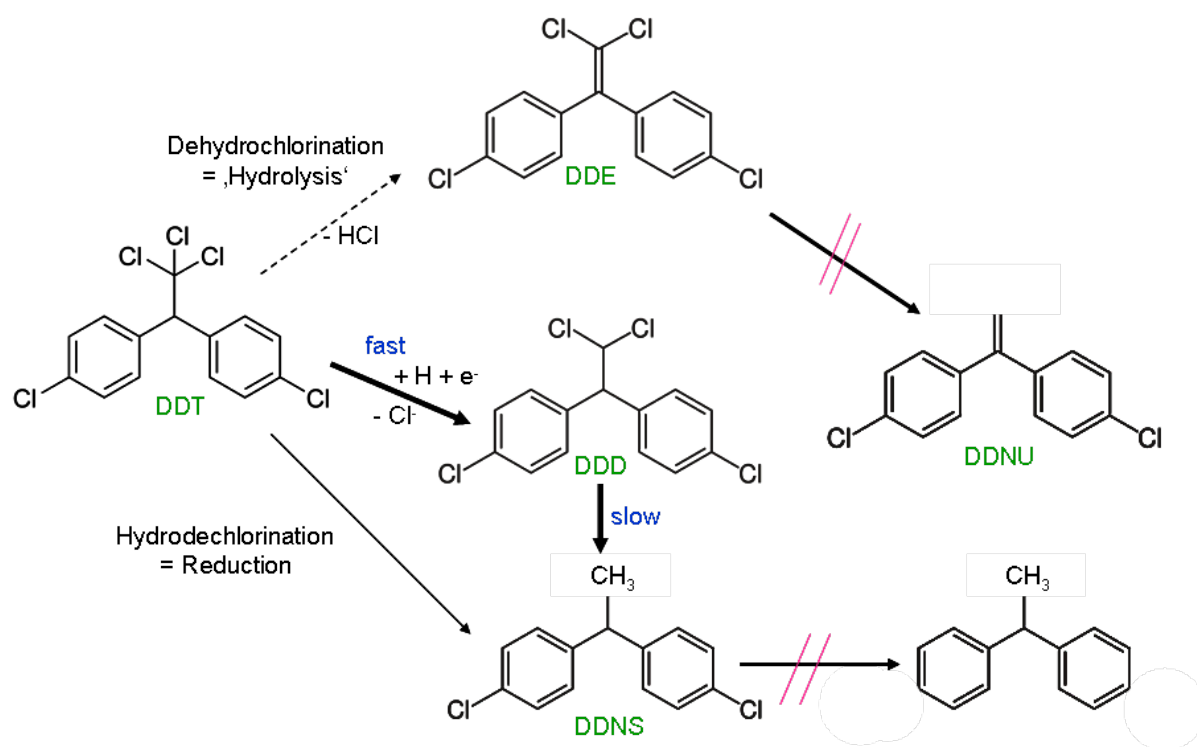
713

714   **Figure 1.** Conversion of DDT adsorbed on FAC (50 mg, 0.5 wt-% DDT) in static contact

715   with µZVI (10 g) under 3 mM NaHCO$_3$ solution (40 mL) as electrolyte (pH = 8.5). One

716   data point (pink circle in the inset) was not included in the regression. The lines are

717   guides for the eye only.

718

719   **Figure 2.** Experimental setup for reaction between DDT adsorbed on FAC and µZVI

720   in a fixed-bed arrangement with two different modes of contact: (i) direct physical

721   contact (right vial), and (ii) electrical contact without physical contact between FAC and

722   µZVI (glass tube and dialysis tubing as separating walls, left vial).

723

724   **Figure 3.** Conversion of DDT loaded on graphite (0.1 wt-%) in aqueous suspension

725   with µZVI ($C_{\mu ZVI}$ = 2 kg L^{-1}, $C_{graphite}$ = 5 g L^{-1}, 3 mM NaHCO$_3$, pH = 8.0). The inset shows

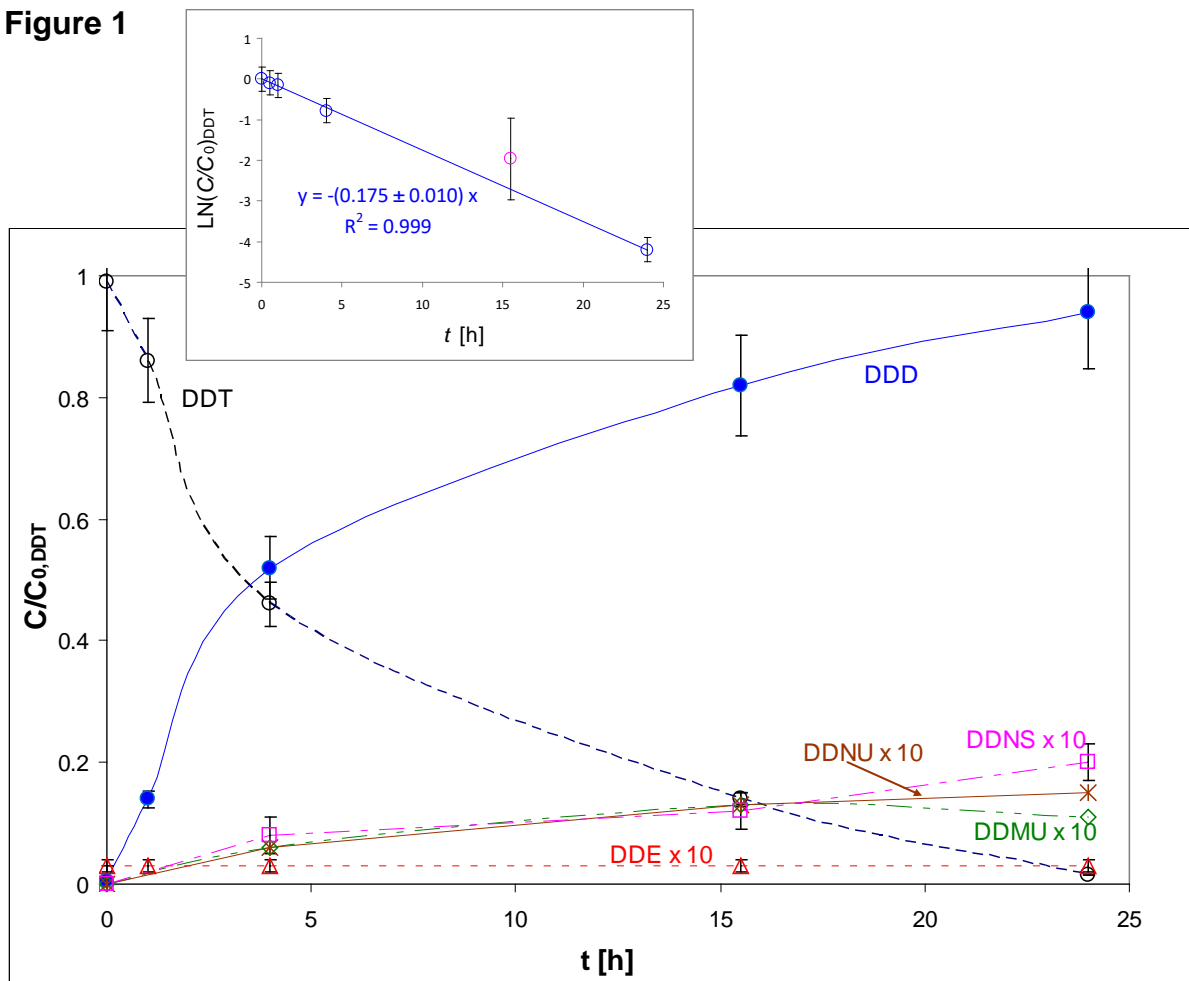726   a semi-logarithmic plot of the DDT conversion kinetics.
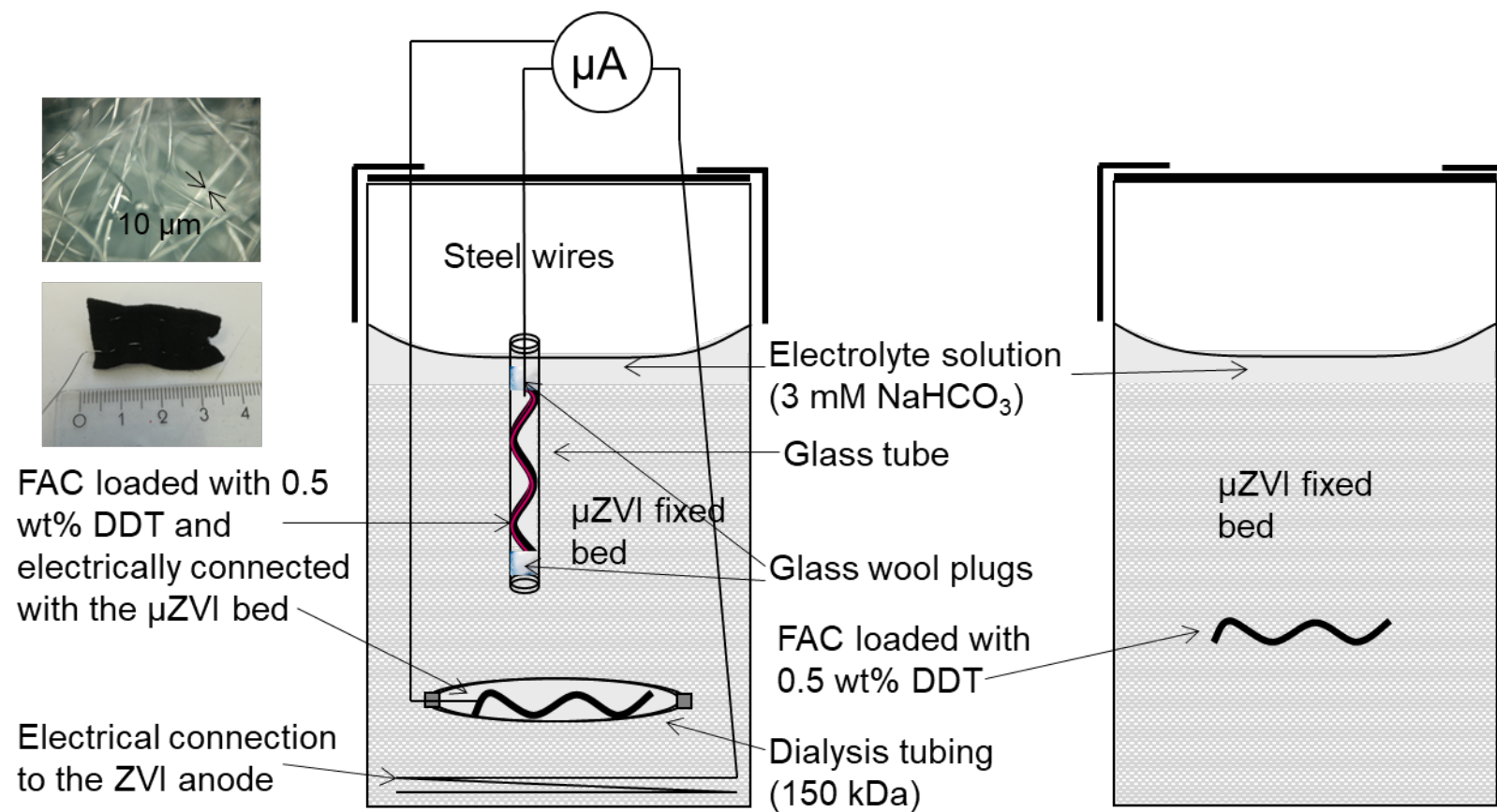
727 **Scheme 1**

Dehydrochlorination
= ‚Hydrolysis‘

- HCl

DDE

DDT

fast
+ H + e⁻
- Cl⁻

Cl Cl

DDD

DDNU

Hydrodechlorination
= Reduction

slow

CH₃

DDNS

CH₃

728

729

730 **Figure 1**

731

732

733

734

735 **Figure 2**

μA

10 µm

Steel wires

Electrolyte solution
(3 mM NaHCO₃)

Glass tube

FAC loaded with 0.5
wt% DDT and
electrically connected
with the µZVI bed

µZVI fixed
bed

Glass wool plugs

FAC loaded with
0.5 wt% DDT

Electrical connection
to the ZVI anode

Dialysis tubing
(150 kDa)

µZVI fixed
bed

736

737

738   **Figure 3**